applied sciences

MDPI

Article

Influence of Ambient Temperature on Optical Characteristics and Power Consumption of LED Lamp for Automotive Headlamp

Chun-Hsin Chang [1], Tun-Ping Teng [1] and Tun-Chien Teng [2,*]

[1] Undergraduate Program of Vehicle and Energy Engineering, National Taiwan Normal University, Taipei 106, Taiwan
[2] Department of Mechatronic Engineering, National Taiwan Normal University, Taipei 106, Taiwan
* Correspondence: walter.teng@ntnu.edu.tw

Abstract: In this study, the authors propose a method for evaluating the influence of ambient temperature (T_a) on the optical characteristics and power consumption of a LED lamp used for the automotive headlamp, which helps the designer to figure out the acceptable range of the ambient temperature for the LED lamps to work well in the practical case. The LED lamp was fixed on the test holder and placed in a fixed position in the air circulation temperature control oven to measure the illuminance, spectrum in three different directions, and power consumption under various T_a. The experimental results indicate that T_a has little effect on the correlated color temperature (CCT), chromaticity coordinates, and angular distribution of the emitting light. In contrast, T_a has a significant effect on the lamp's resistance, thus affecting illuminance and power consumption. When the T_a increased from 30 °C to 60 °C, the illuminance of the low beam and high beam decreased on average by 16.6% and 21.7%, respectively, while the power consumption of the low beam and high beam decreased on average by 21.4% and 22.2%, respectively. The drop in the luminous flux output indicates the probability of originally qualified automotive LED headlamps becoming unqualified in high T_a.

Keywords: headlamp; LED lamp; power consumption; thermal dissipation; color rendering

check for updates

Citation: Chang, C.-H.; Teng, T.-P.; Teng, T.-C. Influence of Ambient Temperature on Optical Characteristics and Power Consumption of LED Lamp for Automotive Headlamp. *Appl. Sci.* **2022**, *12*, 11443. https://doi.org/10.3390/app122211443

Academic Editor: Vincenzo Luigi Spagnolo

Received: 25 September 2022
Accepted: 7 November 2022
Published: 11 November 2022

1. Introduction

Since 2010, car manufacturers have designed high-end vehicles with Light-Emitting Diode (LED) headlamps instead of traditional halogen lamps and high-intensity discharge (HID) bulbs. Halogen bulbs have the advantages of simple manufacturing, low cost, and the capability to illuminate far distances. However, they have disadvantages such as low luminous efficacy, short lifetime, and extremely high temperature. The correlated color temperature (CCT) is about 2600 K to 3200 K. The brightness of HID bulbs is three times that of halogen bulbs, the temperature of the lamp is between 300 °C and 400 °C, and the CCT is between 4000 K and 10,000 K. Both halogen bulbs and HID bulbs have the problem of high temperature. HID bulbs also have the risk of high-voltage electricity [1,2]. In contrast, applying LEDs in automobile headlamps can improve the shortcomings mentioned above and has considerable advantages. Many automobile manufacturers design multi-zone lighting to make vehicles adaptable to various road conditions, such as the matrix LED headlamp of the AUDI [3], the multi-beam LED headlamp of BENZ [4], and the adaptive LED headlamp of BMW [5]. The headlamps can accurately distribute the light to improve safety in driving vehicles according to the various road conditions in urban areas, suburbs, and highways.

The main purpose of using LED lamps in car headlamps is to reduce power consumption and heat generation, extend the bulb's lifetime, increase the illumination level, and meet the requirements of relevant laws and regulations [6–9]. The ambient temperature has a considerable impact on the luminous intensity and lifetime of the LED [10,11]. Using the LED in the headlamp of a car is necessary to understand further the effect of the ambient temperature on the performance of the LED. The headlamps are installed on the left and right sides of the front of the car. Although there is a windward effect of removing the heat during driving, the internal combustion engine (ICE) generates much heat in the engine room. If the ambient temperature is 35 °C, the air temperature in the engine room is as high as 60 °C to 70 °C, and up to 80 °C at most [9]. Such high ambient temperature would significantly impact the performance of the LED chip of the LED headlamp [12,13]. The junction temperature (T_j) of the LED in automobile headlamps is high. Generally, the maximum temperature of T_j is about 150 °C, and the limit on the temperature is 175 °C [14]. The higher ambient temperature is adverse to the heat dissipation of the LED lamps, which causes an increase in T_j and affects the luminous intensity and lifetime of the LED chips [15–18].

In recent years, many researchers have devoted themselves to solving the heat dissipation problem of LED chips through numerical analysis [16,19–21] and experimental methods [22–24] and have achieved remarkable results. Important related references on heat dissipation of vehicle headlights are detailed below. Jung et al. [19] used computational fluid dynamics to develop an air-cooled heat sink for LED headlamps and conducted experiments on a plate-fin type heat sink with a cooling fan for heat dissipation. The experimental results showed that the temperature of the soldering point T_{sp} and the evaluated T_j were 62.8 °C and 103.6 °C, respectively, T_j lower than the maximum acceptable T_j.

Sökmen et al. [16] used ANSYS CFX 14 software to study the effects of fin design, fin materials, natural convection, and forced convection on T_j in the cooling application of LED automotive headlamps under various ambient temperatures (25 °C, 50 °C, and 80 °C) and dissipated powers (0.5 W, 0.75 W, 1 W, and 1.25 W). The research results show that proper fin structures give the best heat dissipation performance for LEDs; the high heat transfer coefficient and copper fins have a positive effect on the T_j of the LED.

Chen et al. [22] used a flexible woven heat sink (FWHS) of copper belts to conduct an experimental study on the heat dissipation performance of LED headlamps under the ambient temperature between 30 °C and 80 °C. The results of the study showed that the overall temperature of the headlamp increased almost linearly with the input power and the ambient temperature. The cooling effect of FWHS was enhanced with the wind speed, and the optimal wind speed was about 2 m/s. At ambient temperature below 50 °C, the total thermal resistance was stably maintained at 4.42 °C/W. However, the total thermal resistance rapidly increased when the ambient temperature exceeded 50 °C, achieving a total thermal resistance of 5.61 °C/W at 80 °C.

Lu et al. [23] developed a three-dimensional vapor chamber (3D VC) device to solve the heat dissipation problem of LED automotive headlamps. This 3D VC included a flattened heat pipe and a circular vapor chamber. The research results showed that both-sides heating had better thermal performance than one-side heating when the total heating load on the 3D VC was the same. The 3D VC had good temperature uniformity and had the lowest thermal resistance of 0.125 °C/W at a 50 W heating load.

Singh et al. [24] used a heat-pipe-based cooling system with piezo fans to improve the heat dissipation of automotive headlamps. The heat pipe had a heat capacity 2–3 times higher than die-cast heat sinks, and the weight was reduced by 50%. The piezo fan blew directly to the LED substrate and generated air convection in the headlamp lampshade. This system improved the heat transfer coefficient of the air and reduced the temperature of the measurement point on the LED substrate by 7.6 °C and increased the heat transfer coefficient of the air in the headlamp enclosure by three times compared with natural convection (5 W/m^2 K increased to 15 W/m^2 K).

The higher T_j of the LED reduced the lifetime of the LED lamp and its illuminance, changed color rendering [25,26], deteriorated the chip package, melted the solder joint, and damaged the chip [27,28]. Therefore, the main purpose of the methods mentioned above for improving heat-dissipation of automotive LED lamps is to reduce T_j to increase the efficiency and lifetime of the LED lamps. However, the ambient temperature directly affects heat dissipation performance, and thus the T_j of the LEDs in lamps, and also affects the power consumption of the LED lamps.

Compared with the research on LED chips, the literature discussing the automotive LED lamp is less. In the references of this paper, only Refs. [13,19,22] have proposed the test method for a whole automotive LED lamp. The method of Ref. [13] is to put an automotive LED lamp on the incubator, let it be in the environment with an ambient temperature of 30 °C~80 °C, and test whether the proposed heat dissipation design can effectively reduce the LED junction temperature. Similarly, Ref. [22] tests the thermal resistance of different heat dissipation designs and the corresponding LED junction temperature. In Ref. [19], an automotive LED lamp is placed at a room temperature of 25 °C. A fixed power of 25 W is input to test the LED junction temperature corresponding to different heat dissipation designs. In addition, the spectrum and angular distribution of light output by the automotive LED lamp are also tested. This study proposed a simple measurement system and method that can simultaneously measure the temperature, power consumption, and optical properties of an automotive LED lamp at different ambient temperatures. The relevant research results and experimental methods would help the designer figure out the acceptable range of the ambient temperature for the LED lamps to work well in the automotive headlight, which is beneficial to designing products that comply with regulations while considering the balance of cost and performance.

2. Lighting Specification for Automotive Headlamps

Concerning traffic safety, the regulation ECE R112 Revision 3 [29] requires that automotive headlamps produce enough illuminance on the road while not illuminating the driver of the oncoming vehicle so as to cause glare [30,31]. Therefore, the headlamp must provide a clear cut-off line in the illuminated zone on the projection screen for vehicle inspection. Figure 1 shows the test points and zones on the projection screen for inspecting the light intensity of the headlamp. During the inspection, the automotive headlamp is 25 m away from the screen, and the screen needs to have enough space to display the light pattern illuminated by the headlamp. The cut-off line is horizontal on the left side of the vv line, and on the right side is the polyline formed by the points HV, H1, H2, and H3. The segment between HV and H1 has a 45° angle to the horizontal, and the segment between H2 and H3 has a 15° angle to the horizontal [29]. To maintain the uniform standard during the inspection, the LED lamp module applies 13.2 V. The ECE R112 regulation emphasizes the light intensity (cd) requirement of the passing beam measured on the screen, which requires the measuring points to comply with their respective specification. The intensity can be calculated from the illuminance on the screen as:

$$I(h,v) = (h,v)r^2/cos\gamma \quad (1)$$

In Equation (1), E_{25m} (h,v) is the illuminance measured at the point on the screen; r is the distance between the headlamp and the measurement point; γ is the projection angle.

Table 1 lists the intensity required for each measurement point on the screen to ensure that the corresponding area on the road has appropriate illuminance, according to Ref. [29]. In the test point angular coordinates, R and L means on the right side and left side of the vv line in Figure 1, respectively; U and D means on the upper side and downside of the hh line in Figure 1, respectively. The headlamp specification is classified into CLASS A and CLASS B, identified by particular photometric provisions. The asymmetrical LED headlamps currently apply to CLASS B. Zone I is the road area close to the vehicle. Zone IV is the farther area from the vehicle, so its minimum intensity must be above 2500 cd to ensure driving safety. Zone III is the area outside the cut-off line of light and dark, and its maximum intensity must not exceed 625 cd to avoid glare on oncoming vehicles. Considering the safety of oncoming vehicles, the maximum intensity of 75L and 50L is limited to 10,600 cd and 13,200 cd, respectively. 75R and 50R are the key points of vehicle lighting, so the regulation requires that the two intensities must be at least 10,100 cd or more; the minimum intensity at 50 V must be greater than 5100 cd. The light aiming 25L and 25R doesn't directly illuminate the oncoming car. However, it needs to illuminate the wide area close to the car for the driver to see the road clearly, so their minimum intensities must be above 1700 cd.

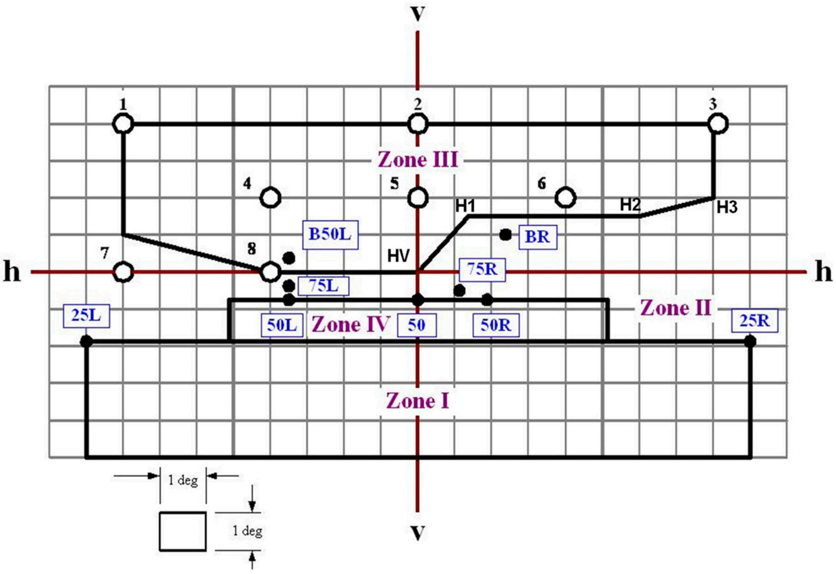

Figure 1. Illustration of test points and zones on the projection screen for inspecting the right-hand traffic passing beam.

Table 1. Luminous intensities at the test points and zones required for the right-hand traffic passing beam.

Headlamps for RH Traffic		**Class A Headlamp**		**Class B Headlamp**	
Test Point Designation	**Test Point Angular Coordinates—Degrees**	**Required LUMINOUS Intensity cd**		**Required Luminous Intensity cd**	
		Max	**Min**	**Max**	**Min**
Point B50L	0.57U, 3.43L	350		350	
BR	1.0U, 2.5R	1750		1750	
Point 75R	0.57D, 1.15R		5100		10,100
Point 75L	0.57D,3.43L	10,600		10,600	
Point 50L	0.86D, 3.43L	13,200		13,200	
Point 50R	0.86D, 1.72R		5100		10,100
Point 50V	0.86D, 0				5100
Point 25L	1.72D, 9.0L		1250		1700
Point 25R	1.72D, 9.0R		1259		1700
Any point in zone III		625		625	
Any point in zone IV			1700		2500
Any point in zone I		17,600		<2I *	

* Actual measured value at points 50R/50L respectively.

According to the above regulations, each area on the screen requires maximal or minimal intensities. In addition to the light shape and the cut-off line requirements, the intensity for each measurement point is important for the car headlamp design. Thus, the luminous flux output from the headlamp must be kept as stable as possible. When the luminous output of the LED chips decreases as the ambient temperature increases, the LED headlamps that originally complied with the regulations may not meet the requirements of the regulations. Therefore, this issue must be considered in advance for designing LED headlamps to ensure that the LED headlamps still comply with the regulations in practical use, which can improve the safety of vehicles.

3. Experimental Design and Implementation

Figure 2 shows the LED lamp used in the automotive headlamps (CCT 6000 K pure white LUXEON; LED-HL [≈H4], PHILIPS, Shanghai, China) was used for testing in this study. Both sides of the lamp have four of the same LED chipsets (a chipset with three LED chips), and each side has two: one for the driving beam (hereafter called high beam) and the other for the passing beam (hereafter called low beam). There is a reflector under the low beam chipset to control the light distribution from the low beam chipset. The electrical specifications of this LED lamp have an input current of 1.2 A and power consumption of approximately 15.5 W when the supply voltage is 13.2 V (for both high beam and low beam). Each side for fixing the LED chipsets on the substrate has an aluminum rivet, and a thermocouple (1/0.2 mm × 2C, T-type, accuracy: ±0.75%) was installed here to measure the temperature of the substrate (T_1). Because of the excellent thermal conductivity of aluminum rivets, the temperature at this point represented the surface temperature of the substrates on both sides. In addition, a thermocouple was installed on the aluminum body (T_2) and the aluminum fin radiator (T_3) to measure the temperature at these locations. Furthermore, two thermocouples (T_4 and T_5) were set up in the test space of the LED lamp to measure the ambient temperature (T_a) of the experiment. All thermocouples used were of the same form.

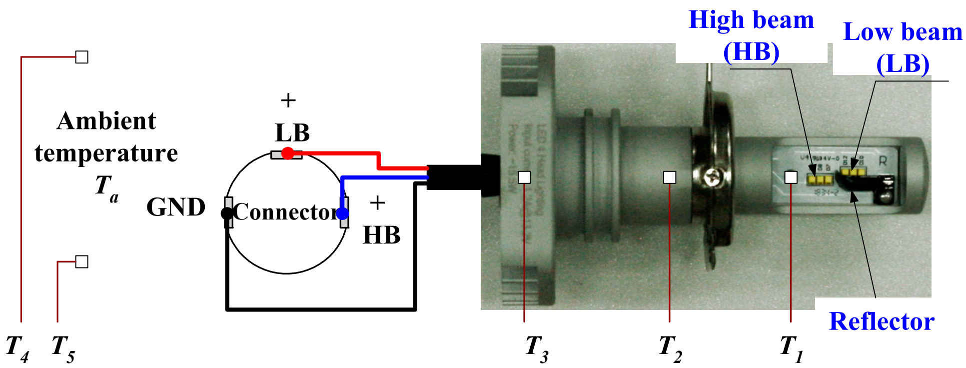

Figure 2. Photograph of automotive LED lamp and schematic diagram of measurement position.

Figure 3 is a schematic diagram of the experimental measurement system. The LED lamp was fixed on the test holder and placed in a fixed position in the air circulation temperature control oven (internal dimensions: W60 × D50 × H50; DH-600N, YOTEC, Hsinchu, Taiwan) to measure the illuminance, spectrum, and power consumption under various T_a (30, 40, 50, and 60 °C). The center of the low beam and high beam chipsets of the LED lamp was aligned with the air vent on the upper side of the oven through which the illuminance spectrum was measured, and the measurement distance was about 305 mm. The illuminance is proportional to the luminous flux, so the authors measured the illuminance to monitor whether the luminous flux changed. To avoid the stray light from the environment entering the measuring instrument, the vent was plugged into a black tube to absorb most of it. The tube has a length of 270 mm and a diameter of 25 mm. The illuminance of the LED lamp was measured by an illuminance meter (LX-103, Lutron, Taipei, Taiwan; accuracy: ±5.0% + 2 digits) six times for each experimental parameter, and the average value was taken as the experimental data. The spectrum of LED lamps from 350 nm to 800 nm was measured using an optic fiber spectrometer (wavelength range: 200~850 nm; BRC112E-V Quest™X, B&W, Plainsboro, NJ, USA) with an integrating sphere (ψ = 5 cm). To inspect the effect of T_a on the angular distribution of the luminous flux and spectrum, the illuminance and spectrum of the LED lamp were measured in three directions of the LED lamp (0, 90, 180 degrees) by rotating the fixture shaft. Referring to the inset in Figure 3, the direction '0 degrees' means rotating the LED lamp to let the LED chips on the right side face the upper air vent (in the y-direction), the direction '180 degrees' means rotating the LED lamp to let the LED chips on the left side face the upper air vent, and the direction '90 degrees' means rotating the LED lamp to let the normal of the LED chips parallel to the x-axis as shown in the current illustration of the inset.

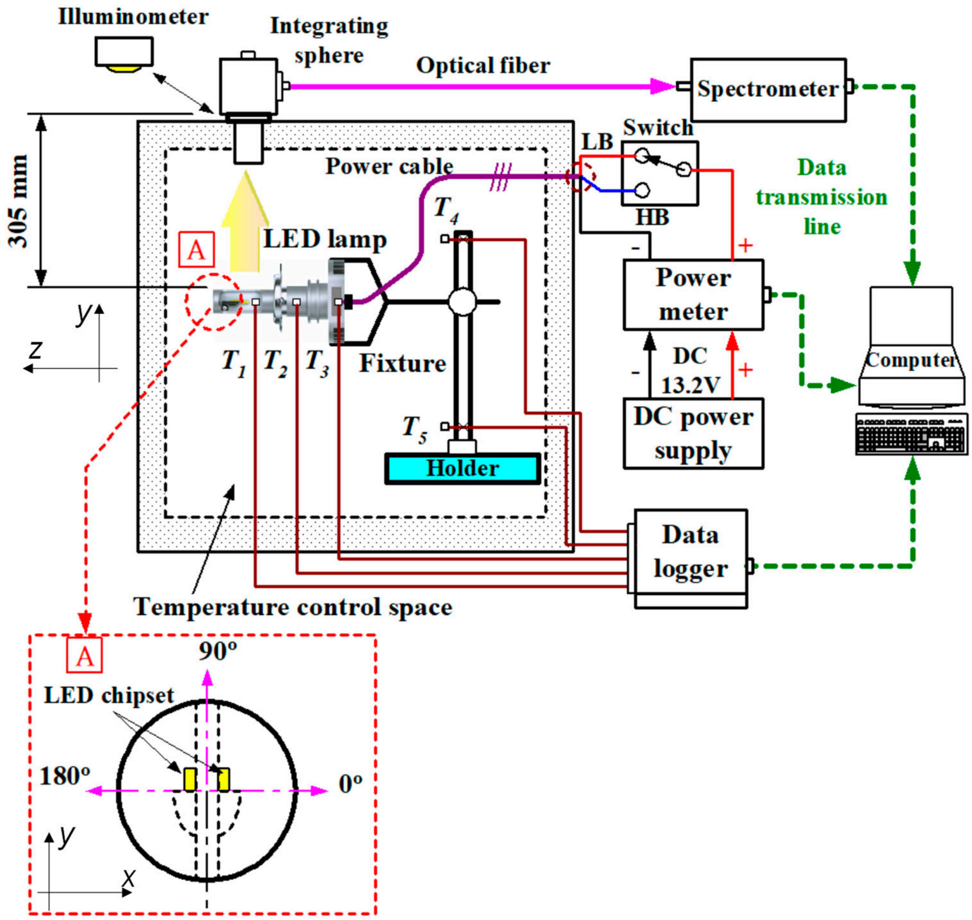

Figure 3. Schematic diagram of the experimental measurement system.

The power supply of the LED lamp used a digital programmable power supply (0–30 V/6 A; PSM-6003, GWINSTEK, New Taipei City, Taiwan; accuracy: ±0.05% + 10 mV/0.2% + 10 mA) with a constant voltage of 13.2 V, and was equipped with a power analyzer (WT230, YOKOGAWA, Tokyo, Japan; accuracy: ±0.2%) that measured and recorded related power data with a sampling time of 5 s. Because this LED lamp was used to replace the halogen bulbs originally installed in car headlights, the authors controlled the fixed voltage of 13.2 V in the experiment according to the actual use situation in which the lamp holders in ordinary cars are powered by constant voltage.

A data logger (TRM20, TOHO, Sagamihara, Japan; accuracy: ±0.1% + 1 digit) was used to measure and record related temperature data with a sampling time of 5 s. The power supply for the high beam and the low beam was switched by a power switch. The experimental conditions included four different temperatures (30, 40, 50, and 60 °C), two lighting forms (low beam and high beam), and three measurement directions (0, 90, and 180 degrees). There were a total of 24 sets of experimental parameters in the experiment. Our pre-test confirmed that the power consumption, illuminance, and temperature of the test point had stabilized after the lamp was turned on for about 6 min at a stable ambient temperature. Therefore, each experimental parameter was continuously implemented for 10 min after the ambient temperature was maintained at the set value. The illuminance and spectrum of the LED lamp were measured after the tenth minute of the initiation of the experiment. The temperature and power consumption of the LED lamp was the average for the last three minutes of the measurement data as the steady-state experimental data (from the seventh to the tenth minute). The ambient temperature (T_a) of the experiment was the average of T_4 and T_5, and this value must be controlled within +2.5 °C of the set value.

This study explored the influence of different T_a on the spectrum, illuminance, and power consumption of LED lamps. Therefore, the relevant experimental data was based on the experimental data with the T_a of 30 °C as the comparison benchmark. As shown in Equation (2), the experimental data of other T_a and the experimental data of the T_a of 30 °C were converted into percentage differences (PD) to facilitate the presentation of the influence of the T_a on the relevant experimental data.

$$PD\% = [(DT_{40\sim60^\circ\mathrm{C}} - DT_{30^\circ\mathrm{C}})/DT_{30^\circ\mathrm{C}}] \times 100\% \quad (2)$$

4. Results and Discussion

Figure 4a–c shows the spectral measurement results of LED lamps at three illumination angles 0°, 90°, and 180°, respectively. Each figure contains the measurement results of two types of LED chipsets (low beam (L) and high beam (H)); each type of LED chipset was measured under four ambient temperatures of 30, 40, 50, and 60 °C, respectively. Figure 4 indicates that the spectral distribution of the LED lamp under various conditions was very similar, and its spectral intensity decreased with the ambient temperature T_a. The illumination angles of 0° and 180° mean that the LED chips on the right and left sides, respectively, faced the measuring hole (vent). Therefore, the received luminous flux for the illumination angles of 0° and 180° is higher than 90°. The spectral intensity of the high beam is much higher than that of the low beam for the illumination angles of 0° and 180°. However, the spectral intensity of the high beam is lower than that of the low beam for the illumination angle of 90°. It is because part of the light of the low beam LED chipsets was reflected in the 90°direction by the reflector, while most of the light of the high beam LED chipsets was emitted toward the directions of 0° and 180°.

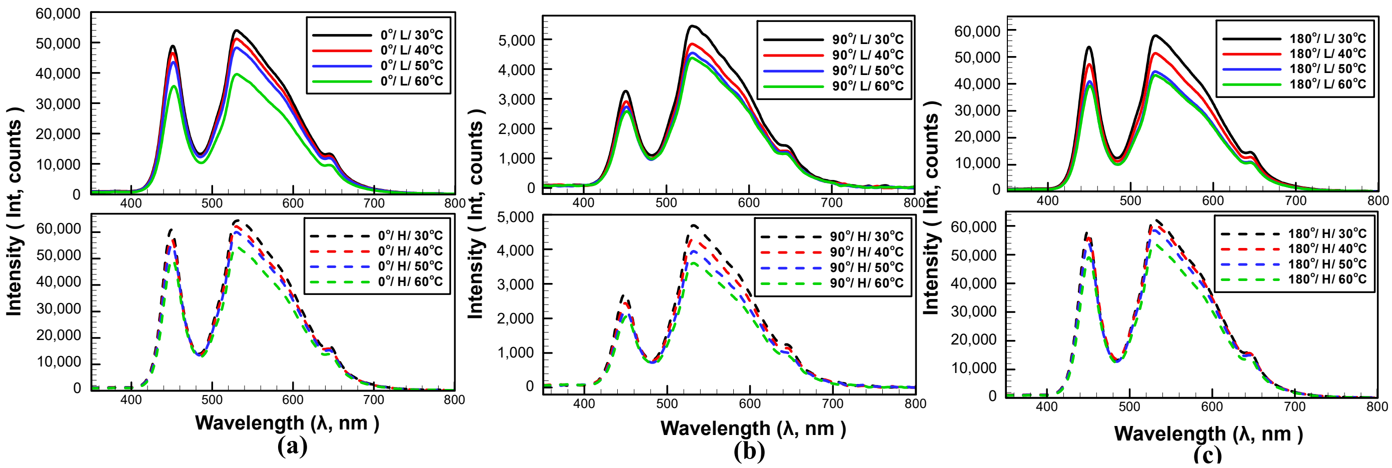

Figure 4. Spectral measurement results of the LED lamp: (**a**) 0°, (**b**) 90°, and (**c**) 180°.

To evaluate the effect of the temperature on relative spectral distribution, the data on each curve in Figure 4 are divided by the maximum value on that curve and multiplied by 100 to form Figure 5. Figure 5 indicates all the normalized spectral distributions of different T_a almost coincided, which means that the temperature had little effect on the color rendering of the light. In general, the higher junction temperature causes the dominant wavelength to drift higher, e.g., ~0.1 nm/°C for an InGaAlP LED. In the experiment, the raw data of the measured spectrum indicate the drift of the peak wavelength of the blue light was about 1~1.5 nm. Such a small drift can hardly be observed in Figures 4 and 5. To further inspect the change in the color rendering, the spectral data of the LED lamps in Figure 4 can be further calculated into the CCT, Duv, and chromaticity coordinates (CIE x, y) shown in Table 2, which shows that the T_a had little effect on the CCT, Duv, and chromaticity coordinates in the short-term test regardless of illumination angles, high beam, or low beam [32]. In addition, the CCT of the high beam and low beam of LED lamps at the illumination angles of 0° and 180° was very close to the original specifications of the LED lamps (CCT 6000 K). However, the CCT at the illumination angle of 90° was significantly lower than 6000 K, mainly because of the color unevenness of the light emitted from the LED chips in the angular space. In general, slanted light from the white-light LED at a large angle with a normal emitting area tended to be yellowish (lower CCT) [33]. The low beam of the LED lamp measured at an illumination angle of 90° included the slanted light and the reflected light that was originally toward the normal around by the reflector, and the high beam of the LED lamp measured at an illumination angle of 90° only included the slanted light. Therefore, the high beam of the LED lamp measured at an illumination angle of 90° displayed a lower CCT than the low beam of the LED lamp.

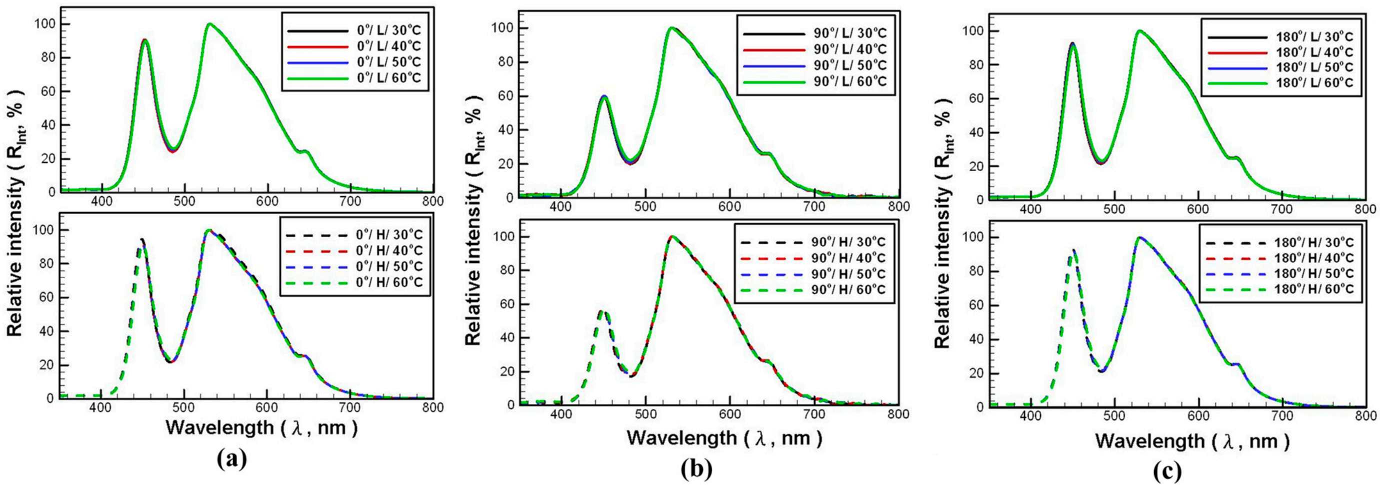

Figure 5. Normalized spectral measurement results of the LED lamp: (**a**) 0°, (**b**) 90°, and (**c**) 180°.

Table 2. Correlated Color temperature (CCT), Duv, and chromaticity coordinates of the LED lamp.

Deg. (°)	T_a (°C)	Low Beam				High Beam			
		CCT		CIE 1931 xy		CCT		CIE 1931 xy	
		K	Duv	CIE x	CIE y	K	Duv	CIE x	CIE y
0	30	5949	0.0319	0.3191	0.3981	5835	0.0304	0.3225	0.3978
	40	5963	0.0321	0.3187	0.3981	5854	0.0309	0.3219	0.3983
	50	5981	0.0324	0.3181	0.3981	5860	0.0309	0.3217	0.3983
	60	6005	0.0325	0.3174	0.3978	5875	0.0312	0.3213	0.3985
90	30	5284	0.0389	0.3415	0.4379	5211	0.0398	0.3447	0.4433
	40	5315	0.0392	0.3403	0.4375	5203	0.0397	0.3450	0.4433
	50	5306	0.0398	0.3407	0.4376	5219	0.0398	0.3443	0.4429
	60	5311	0.0388	0.3404	0.4367	5234	0.0396	0.3437	0.4416
180	30	5881	0.0312	0.3211	0.3983	5843	0.0307	0.3223	0.3984
	40	5899	0.0316	0.3205	0.3986	5840	0.0309	0.3223	0.3989
	50	5926	0.0316	0.3198	0.3981	5850	0.0310	0.3220	0.3988
	60	5922	0.0317	0.3199	0.3983	5867	0.0312	0.3215	0.3988

Table 3 lists the illuminance, power consumption, and lighting efficiency of the LED lamp. The illuminance decreased with the T_a, which has the same trend as the spectral intensity. In addition, the power consumption decreased with the increase in the T_a. When the T_a increased from 30 °C to 60 °C, the illuminance of the low beam and high beam at illumination angles of 0°, 90°, and 180° decreased by 15.7%, 14.9%, and 19.2%, and 24.1%, 20.1%, and 21.0%, respectively. When the T_a increased from 30 °C to 60 °C, the power consumption of the low beam and high beam with illumination angles of 0°, 90°, and 180° decreased by 21.7%, 21.2%, and 21.3%, and 22.5%, 22.5%, and 21.6%, respectively. The illuminance is proportional to the luminous flux output, so the luminous flux output decreased with T_a. This study combined the illuminance and power consumption of the LED lamp to further define the lighting efficiency (*LEF*, lx/W) as the illuminance generated per unit of power consumption. The experimental results showed that increasing T_a caused the *LEF* of the LED lamp to fluctuate a little, which is not the same as the situation where high temperature reduces the optical efficiency of the LED chips. When the LED lamp was powered by a constant voltage, the rise of ambient temperature increased the resistance of the lamp and thus reduced the current injected into the LED chips, leading to low luminous output. Although higher temperature decreases the optical efficiency of LED chips, the reduced injection current to LED chips benefits the LEF [34]. Because these two-factor effects substantially canceled each other out, the LEF only varied from −6.2% to 8% with the increase in the ambient temperature. The drop in the luminous output is mainly attributed to the increase in resistance of peripheral electronic devices of the LED lamp with the ambient temperature, instead of the generally expected factor where the optical efficiency of the LED decreases with the junction temperature.

Table 3. Illuminance, power consumption, and lighting efficiency of the LED lamp.

Deg. (°)	T_a (°C)	Low Beam						High Beam					
		Illuminance		Power Consumption		LEF		Illuminance		Power Consumption		LEF	
		lx	PD%	W	PD%	lx/W	PD%	lx	PD%	W	PD%	lx/W	PD%
0	30	2795.0	—	13.71	—	203.8	—	3226.7	—	14.30	—	225.6	—
	40	2695.0	−3.6	12.72	−7.2	211.8	3.9	2961.7	−8.2	13.20	−7.7	224.4	−0.5
	50	2511.7	−10.1	11.59	−15.5	216.8	6.4	2566.7	−20.5	12.12	−15.2	211.7	−6.2
	60	2356.7	−15.7	10.74	−21.7	219.5	7.7	2448.3	−24.1	11.09	−22.5	220.8	−2.1
90	30	276.3	—	13.65	—	20.2	—	215.0	—	14.39	—	14.9	—
	40	265.7	−3.9	12.66	−7.3	21.0	3.7	197.5	−8.1	13.13	−8.8	15.0	0.7
	50	240.2	−13.1	11.68	−14.4	20.6	1.6	184.2	−14.3	12.06	−16.2	15.3	2.2
	60	235.2	−14.9	10.76	−21.2	21.9	8.0	171.8	−20.1	11.15	−22.5	15.4	3.2
180	30	2318.3	—	13.65	—	169.9	—	2980.0	—	14.18	—	210.2	—
	40	2101.7	−9.3	12.69	−7.0	165.6	−2.5	2843.3	−4.6	13.01	−8.2	218.5	4.0
	50	2001.7	−13.7	11.64	−14.7	172.0	1.2	2656.7	−10.9	12.12	−14.5	219.2	4.3
	60	1873.3	−19.2	10.73	−21.3	174.5	2.7	2355.0	−21.0	11.11	−21.6	212.0	0.9

Generally, an LED lamp is used in a closed lampshade for the automotive headlamp. Qualified automotive headlamps must meet the specifications regarding light distribution and intensities of the sampling points in the bright and dark areas [29]. However, if the luminous flux output of the LED lamps decreases at high T_a, the originally qualified automotive LED headlamps would probably become unqualified, especially in the hot-weather area or in vehicles with the internal combustion engine. Although raising the rated power consumption of the LED lamps to guarantee sufficient luminous flux output in the hot environment is intuitive, it would lead to energy waste and probably cause the intensities of some areas to exceed the maximal limit of the specifications, making the design of LED headlamps more difficult. Automotive LED headlights must have a total solution. Potential feasible ways include strengthening the heat dissipation of the whole LED lamp, adopting additional feedback circuits to ensure stable luminous output, and enhancing the thermal management of the entire headlight module for blocking the heat from the engine room and dissipating the heat from the LED lamp.

Table 4 lists the temperature and temperature differences of each point of the LED lamp under different experimental conditions. Overall, the temperature of each point increased with T_a. In addition, the rising rate of the temperature of the measurement point farther away from the LED chipsets was more affected by increasing the T_a. In other words, the T_a has the least influence on the temperature of the substrate of the LED chipsets (T_1) but has the greatest influence on the aluminum fin radiator (T_3). This phenomenon is primarily because the effective contact area between the substrate of the LED chipsets and the surrounding ambient air was small. The heat dissipation of the substrate of the LED chipsets was mainly through the aluminum body to the aluminum fin radiator and then to the surrounding air. The heat transfer of the LED lamp to the surrounding ambient air mainly relied on the aluminum fin radiator with a high specific surface area. Therefore, the temperature of the aluminum fin radiator is most significantly affected by T_a.

Under the same experimental condition, the temperature difference between T_3 and T_a was the largest, indicating that the thermal resistance between the aluminum fin radiator and the surrounding air is the largest. The second large temperature difference was between T_1 and T_2 because there was large thermal resistance between the substrate of the LED chipsets and the aluminum body. The smallest temperature difference was between T_2 and T_3 because the aluminum body and the aluminum fin heat sink were tightly connected by threads, and so had very low contact thermal resistance. From the above experimental results, two potential methods can be considered to improve the heat dissipation performance of LED lamps according to the literature. First, the heat transfer performance needs to be strengthened between the substrate of LED chipsets and the aluminum body to reduce the contact thermal resistance by thermal interface materials with high thermal conductivity or reinforcing surface contact [35–39]. Second, thermal resistance could be reduced between the aluminum fin radiator and the surrounding air by using an aluminum fin radiator with a higher specific surface area, heat dissipation coatings with low thermal resistance, and forced circulation air cooling [16,19,23,24,40–42]. Our method can be easily applied to various LED lamps to effectively check whether the LED lamp can work well in higher T_a and find where the LED lamp should be improved regarding heat dissipation by evaluating the temperature at each point.

Relative uncertainty (U_e, %) analysis was performed by calculating the deviations (e) generated by the sensors, measuring instruments, and controllers. The U_e of the ambient temperature came from the deviations of a temperature controller (accuracy: $\pm 0.3\%$) and K-type thermocouple (accuracy: $\pm 0.75\%$) in the air circulation temperature control oven. According to the standard U_e analysis of Equation (3), the U_e of the ambient temperature control was calculated as 0.81%. The U_e was calculated using Equation (3) for temperature (T-type), temperature difference (T-type), illuminance, power consumption, and LEF, which were 1.11%, 1.34%, 5.06%, 0.83%, and 5.07%, respectively, including the U_e of ambient temperature control.

$$U_e = \sqrt{e_1^2 + e_2^2 + e_3^2 + \ldots\ldots\ldots + e_{n-1}^2 + e_n^2 +} \times 100\% \tag{3}$$

Table 4. Temperature measurement results of the LED lamp.

Deg. (°)	T_a* (°C)	Low Beam										High Beam									
		T_1 (°C)	T_2 (°C)	T_3 (°C)	T_a** (°C)	PD$_{T1}$ (%)	PD$_{T2}$ (%)	PD$_{T3}$ (%)	T_1–T_2 (°C)	T_2–T_3 (°C)	T_3–T_a (°C)	T_1 (°C)	T_2 (°C)	T_3 (°C)	T_a** (°C)	PD$_{T1}$ (%)	PD$_{T2}$ (%)	PD$_{T3}$ (%)	T_1–T_2 (°C)	T_2–T_3 (°C)	T_3–T_a (°C)
0	30	78.8	66.3	58.3	31.0	—	—	—	12.5	8.0	27.3	75.9	63.8	56.4	31.2	—	—	—	12.1	7.4	25.2
	40	84.7	73.2	65.9	42.3	7.5	10.4	12.9	11.5	7.3	23.6	82.0	71.1	64.3	41.8	8.1	11.4	13.9	11.0	6.8	22.5
	50	91.2	80.9	74.3	51.9	15.7	22.0	27.4	10.3	6.6	22.4	88.3	78.2	72.1	50.7	16.3	22.7	27.9	10.0	6.1	21.4
	60	96.4	87.1	81.1	61.5	22.4	31.3	39.1	9.4	5.9	19.7	94.2	85.3	79.8	60.6	24.1	33.7	41.4	8.9	5.5	19.2
90	30	78.3	66.0	58.2	31.5	—	—	—	12.3	7.8	26.7	73.9	61.5	54.2	30.7	—	—	—	12.4	7.3	23.5
	40	84.0	72.8	65.7	41.3	7.3	10.2	12.9	11.2	7.1	24.4	81.5	70.7	64.2	41.5	10.2	15.0	18.4	10.8	6.6	22.7
	50	89.9	79.6	73.3	52.0	14.8	20.6	25.8	10.3	6.3	21.3	87.8	78.0	72.2	51.4	18.7	26.9	33.1	9.7	5.9	20.8
	60	95.9	86.5	80.8	61.2	22.4	31.0	38.8	9.4	5.7	19.6	93.5	84.5	79.3	60.6	26.4	37.4	46.2	8.9	5.3	18.7
180	30	79.5	66.1	58.2	31.0	—	—	—	13.4	7.8	27.2	76.6	63.7	56.4	31.3	—	—	—	12.9	7.3	25.1
	40	85.4	73.0	65.7	42.0	7.5	10.4	12.8	12.4	7.3	23.7	83.4	71.7	65.1	42.0	8.9	12.6	15.4	11.7	6.6	23.0
	50	91.7	80.5	73.9	52.3	15.5	21.7	26.8	11.3	6.6	21.6	89.0	78.3	72.1	52.0	16.2	22.9	28.0	10.8	6.1	20.2
	60	97.4	87.1	81.1	61.5	22.7	31.6	39.2	10.3	6.0	19.6	95.0	85.2	79.7	61.1	24.0	33.8	41.3	9.8	5.5	18.6

Note: T_a* is the set value of the ambient temperature, and T_a** is the measured value of the ambient temperature (average of T_4 and T_5).

5. Conclusions

In this study, the authors proposed a simple but effective test method for evaluating the influence of ambient temperature on the optical characteristics and power consumption of a commercial LED lamp used for the automotive headlamp. The experimental results of the LED lamp powered by a constant voltage indicated that the T_a has little effect on the CCT, chromaticity coordinates, and the angular distribution of the emitting light. In contrast, T_a has a significant effect on both illuminance and power consumption. When the T_a rose from 30 °C to 60 °C, the illuminance of the low beam and high beam averagely decreased by 16.6% and 21.7%, respectively, and the power consumption of the low beam and high beam averagely decreased by 21.4% and 22.2%, respectively. The drop in the luminous flux output would probably disqualify the originally qualified automotive LED headlamps. The drop in the luminous output is mainly attributed to the increase in resistance of peripheral electronic devices of the LED lamp with the ambient temperature. Therefore, the heat dissipation of automotive LED headlamps must be considered to effectively mitigate the influence of high T_a on not only LED chips but also the increase in resistance of the LED lamps when designing the related cooling components. In addition, a current-stabilization device might be adopted to ensure stable luminous output. Our method can easily be applied to various LED lamps to effectively check whether the LED lamp can work well in higher T_a and find where the LED lamp should be improved regarding heat dissipation by evaluating the temperature at each point. According to the influence of an increase in T_a on the luminous flux output of the LED lamp, the maximal acceptable T_a can be evaluated. Thus, the designer can select an appropriate solution for the LED headlamp by considering the balance between performance and cost.

Author Contributions: Conceptualization, C.-H.C. and T.-C.T.; designed the experiment, C.-H.C., T.-P.T. and T.-C.T.; carried out the measurements, C.-H.C. and T.-P.T.; analyzed the measurements T.-P.T. and T.-C.T.; wrote and revised the paper, T.-C.T. All authors have read and agreed to the published version of the manuscript.

Funding: This work was partly supported by the Ministry of Science and Technology of the Republic of China (Taiwan) under Contract no. MOST 107-2221-E-003-015-MY3, MOST 110-2221-E-003-008-MY3, MOST 110-2221-E-003-009-MY3.

Institutional Review Board Statement: Not applicable.

Informed Consent Statement: Not applicable.

Data Availability Statement: Not applicable.

Conflicts of Interest: The authors declare no conflict of interest.

References

1. ICECAT, Philips Car Headlight Bulb, H4 Datasheet. 2018. Available online: https://objects.icecat.biz/objects/mmo_56674787_1575761387_8657_14018.pdf (accessed on 1 September 2022).
2. Denton, T. *Automobile Electrical and Electronic Systems*, 4th ed.; Routledge: London, UK, 2013.
3. Audi Website, Audi Matrix LED Headlights, Self-Study Program 619. Available online: https://procarmanuals.com/vag-ssp-619-audi-matrix-led-headlights (accessed on 1 September 2022).
4. Headlamps in the New Mercedes-Benz E-Class: MULTIBEAM LED. Available online: https://youtu.be/0OJjvYPV3oc (accessed on 1 September 2022).
5. BMW Website. Available online: https://www.bmw.com.bn/en/topics/offers-and-services/accessories-pages/bmw-accessory-showroom.bmw-adaptive-led-headlights.html (accessed on 1 September 2022).
6. Ma, S.H.; Lee, C.H.; Yang, C.H. Achromatic LED-based projection lens design for automobile headlamp. *Optik* **2019**, *191*, 89–99. [CrossRef]
7. Zhu, Z.; Wei, S.; Liu, R.; Hong, Z.; Zheng, Z.; Fan, Z.; Ma, D. Freeform surface design for high-efficient LED low-beam headlamp lens. *Opt. Commun.* **2020**, *477*, 126269. [CrossRef]
8. Nair, G.B.; Dhoble, S.J. A perspective perception on the applications of light-emitting diodes. *Luminescence* **2015**, *30*, 1167–1175. [CrossRef]

9. Luce, T. LED headlamps: The spiny path to a legal headlamp. In Proceedings of the European Workshop on Photonics in the Automobile, Geneva, Switzerland, 29 November 2004. [CrossRef]
10. Yao, Q.; Hu, P.; Sun, P.; Liu, M.; Dong, R.; Chao, K.; Liu, Y. Laser-driven solid-state light sources. *Adv. Mater.* **2020**, *32*, 1907888. [CrossRef] [PubMed]
11. Narendran, N.; Gu, Y.; Jayasinghe, L.; Freyssinier, J.P.; Zhu, Y. Long-term performance of white LEDs and systems. In Proceeding of First International Conference on White LEDs and Solid State Lighting, Tokyo, Japan, 26–30 November, 2007; pp. 174–179.
12. Senawiratne, J.; Chatterjee, A.; Detchprohm, T.; Zhao, W.; Li, Y.; Zhu, M.; Xia, Y.; Li, X.; Plawsky, J.; Wetzel, C. Junction temperature, spectral shift, and efficiency in GaInN-based blue and green light emitting diodes. *Thin Solid Film.* **2010**, *518*, 1732–1736. [CrossRef]
13. Wang, J.; Cai, Y.X.; Li, X.H.; Zhao, X.J.; Zhang, C. Design of automotive headlamp with high-power LEDS. *Int. J. Automot. Technol.* **2014**, *15*, 673–681. [CrossRef]
14. Osram Ostar Headlamp, Datasheet Version 1.2. Available online: https://www.digikey.com/en/products/detail/osram-opto-semiconductors-inc/LE-UW-D1W3-01-5P7P-JM-T01-VAR/10423891 (accessed on 1 September 2002).
15. Raypah, M.E.; Devarajan, M.; Sulaiman, F. Influence of injection current and ambient temperature on intensity and wavelength of low-power SMD LED. In Proceedings of the 2016 IEEE 37th International Electronics Manufacturing Technology (IEMT) & 18th Electronics Materials and Packaging (EMAP) Conference, Georgetown, Malaysia, 20–22 September 2016; pp. 1–6.
16. Sökmen, K.F.; Yürüklü, E.; Yamankaradeniz, N. Computational thermal analysis of cylindrical fin design parameters and a new methodology for defining fin structure in LED automobile headlamp cooling applications. *Appl. Therm. Eng.* **2016**, *94*, 534–542. [CrossRef]
17. Xi, Y.; Schubert, E.F. Junction-temperature measurement in GaN ultraviolet light-emitting diodes using diode forward voltage method. *Appl. Phys. Lett.* **2004**, *85*, 2163–2165. [CrossRef]
18. Canale, L.; Dupuis, P.; Leng, S.; Zissis, G. Study of high-brightness led samples aged under stress temperature conditions: Electrical characterizations and signature evolution analysis. *IEEE Trans. Ind. Appl.* **2016**, *52*, 502–510. [CrossRef]
19. Jung, E.D.; Lee, Y.L. Development of a heat dissipating LED headlamp with silicone lens to replace halogen bulbs in used cars. *Appl. Therm. Eng.* **2015**, *86*, 143–150. [CrossRef]
20. Abdelmlek, K.B.; Araoud, Z.; Canale, L.; Charrada, K.; Zissis, G. Optimal substrate design for thermal management of high power multi-chip LEDs module. *Optik* **2021**, *242*, 167179. [CrossRef]
21. Abdelmlek, K.B.; Araoud, Z.; Canale, L.; Nejma, F.B.; Charrada, K.; Zissis, G. Thermal management of LEDs packages within inclined enclosures for lighting applications. In Proceedings of the 2021 IEEE Industry Applications Society Annual Meeting (IAS), Vancouver, BC, Canada, 10–14 October 2021; pp. 1–6.
22. Chen, S.; Chen, K.; Li, Z.; Tang, Y.; Zhuang, B.; Zhong, G.; Liang, G. Experimental investigation on the thermal performance of a light emitting diode headlamp with a flexible woven heat sink. *Appl. Therm. Eng.* **2017**, *127*, 1215–1222. [CrossRef]
23. Lu, Z.; Bai, P.; Huang, B.; Henzen, A.; Coehoorn, R.; Liao, H.; Zhou, G. Experimental investigation on the thermal performance of three-dimensional vapor chamber for LED automotive headlamps. *Appl. Therm. Eng.* **2019**, *157*, 113478. [CrossRef]
24. Singh, R.; Mochizuki, M.; Yamada, T.; Nguyen, T. Cooling of LED headlamp in automotive by heat pipes. *Appl. Therm. Eng.* **2020**, *166*, 114733. [CrossRef]
25. Sivak, M.; Schoettle, B.; Flannagan, M. LED headlamps: Glare and colour rendering. *Light. Res. Technol.* **2004**, *36*, 295–303. [CrossRef]
26. Lee, H.S.; Park, H.J.; Kwak, J.S. Improvement of disturbing color effects depending on the axial color of an automotive headlamp lens. *Appl. Opt.* **2017**, *56*, 5106–5111. [CrossRef]
27. Khandekar, S.; Sahu, G.; Muralidhar, K.; Gatapova, E.Y.; Kabov, O.A.; Hu, R.; Luo, X.; Zhao, L. Cooling of high-power LEDs by liquid sprays: Challenges and prospects. *Appl. Therm. Eng.* **2021**, *184*, 115640. [CrossRef]
28. Wu, Q.; Liang, C.; Huang, L. Thermal design and simulation of LEDs automotive headlamps. In Proceedings of the 21st International Conference on Electronic Packaging Technology (ICEPT), Guangzhou, China, 12–15 August 2020.
29. ECE. *ECE R112 Revision 3*; United Nations Economic Commission for Europe: Geneva, Switzerland, 2013.
30. Long, X.; He, J.; Zhou, J.; Fang, L.; Zhou, X.; Ren, F.; Xu, T. A review on light-emitting diode based automotive headlamps. *Renew. Sust. Energ. Rev.* **2015**, *41*, 29–41. [CrossRef]
31. Wu, H.; Zhang, X.; Ge, P. Modular design of a high-efficiency LED headlamp system based on freeform reflectors. *Opt. Laser Technol.* **2015**, *72*, 79–85. [CrossRef]
32. Supronowicz, R.; Fan, J.; Listowski, M.; Watras, A.; Fryc, I. Application of different metrics for describing light color quality of white LED. *Photonics Lett. Pol.* **2021**, *13*, 31–33. [CrossRef]
33. Kim, W.; Kim, T.; Kim, S.; Yoon, S.; Jeong, H.; Song, J.; Seong, T. Improved angular color uniformity and hydrothermal reliability of phosphor-converted white light-emitting diodes by using phosphor sedimentation. *Opt. Express* **2018**, *26*, 28634–28640. [CrossRef]
34. Raypah Muna, E.; Mutharasu, D.; Fauziah, S. Evaluation of current and temperature effects on optical performance of InGaAlP thin-film SMD LED mounted on different substrate packages. *Chin. Phys. B* **2017**, *26*, 078503. [CrossRef]
35. Rad, S.D.; Islam, A.; Alnasser, A. Development of metal–graphene-filled hybrid composites: Characterization of mechanical, thermal, and electrical properties. *J. Compos. Mater.* **2018**, *53*, 3363–3376. [CrossRef]
36. Lee, S.; Suh, D.; Kim, W.; Xu, C.; Kim, T.; Song, C.; Yoo, C.; Kim, Y.; Kim, J.; Baik, S. Carbon nanotube covalent bonding mediates extraordinary electron and phonon transports in soft epoxy matrix interface materials. *Carbon* **2020**, *157*, 12–21. [CrossRef]

37. Yang, C.R.; Chen, C.D.; Cheng, C.; Shi, W.H.; Chen, P.H.; Teng, T.P. Thermal conductivity enhancement of AlN/PDMS composites using atmospheric plasma modification techniques. *Int. J. Therm. Sci.* **2020**, *155*, 106431. [CrossRef]
38. Suresh, V.; Jegan, A.; Mohan, R.; Mahendran, A.; Gokulanathan, L. Experimental study of heat transfer rate in a stainless steel heating element using nano coating. *Mater. Today Proc.* **2021**, *37*, 3743–3746. [CrossRef]
39. Bahru, R.; Zamri, M.F.M.A.; Shamsuddin, A.H.; Shaari, N.; Mohamed, M.A. A review of thermal interface material fabrication method toward enhancing heat dissipation. *Int. J. Energy Res.* **2021**, *45*, 3548–3568. [CrossRef]
40. Ng, E.C.J.; Kueh, T.C.; Wang, X.; Soh, A.K.; Hung, Y.M. Anomalously enhanced thermal performance of carbon-nanotubes coated micro heat pipes. *Energy* **2021**, *214*, 118909. [CrossRef]
41. Hadi, M.; Ismael, M.A.; Alhattab, H.A. Experimental investigation of thermal performance of the graphene-coated Al heat sink. *Mater. Today: Proc.* **2021**, *42*, 2779–2784. [CrossRef]
42. Ghasemiasl, R.; Taheri, M.A.; Molana, M.; Raoufi, N. Experimental investigation of thermal performance of the graphene oxide coated plates. *Heat Transfer–Asian Res.* **2020**, *49*, 519–532. [CrossRef]